Cement & Concrete Composites 32 (2010) 617–622

Contents lists available at ScienceDirect

Cement & Concrete Composites

journal homepage: www.elsevier.com/locate/cemconcomp

Use of granite sludge wastes for the production of coloured cement-based mortars

I. Mármol [a], P. Ballester [a], S. Cerro [b], G. Monrós [b], J. Morales [c], L. Sánchez [c,*]

[a] Cementos Kola S.A. (CEMKOSA), Avda. Agrupación Córdoba No. 17, Córdoba, Spain
[b] Departamento de Química Inorgánica y Orgánica, Universidad Jaume I, 12071 Castellón, Spain
[c] Departamento de Química Inorgánica, Facultad de Ciencias, Universidad de Córdoba, Campus de Rabanales, Edificio Marie Curie, 14071 Córdoba, Spain

ARTICLE INFO

Article history:
Received 23 February 2010
Received in revised form 7 June 2010
Accepted 16 June 2010
Available online 19 June 2010

Keywords:
Mortar
Granite wastes
Ceramic pigment
Mechanical properties
Colour

ABSTRACT

The value of granite sludge wastes (GS) in cement-based mortar formulations was examined by assessing their potential as structural components and pigments. Full characterization of GS was accomplished by X-ray fluorescence (XRF), X-ray diffraction (XRD), laser diffraction and scanning electron microscopy. GS were found to be an effective filler or pozzolanic material for mortars. Also, GS were easily converted into a reddish pigment by calcination at low temperatures (700–900 °C) for a short time. UV–Vis–NIR spectra, colourimetric parameters and XRD analysis confirmed the presence of α-Fe_2O_3 in the pigment. Therefore, the preparation of coloured mortar with good compressive strength can be an attractive, environmentally friendly method of managing granite sludge wastes.

1. Introduction

Appropriate waste management is one of the main requisites for sustainable development at present. A number of small and large enterprises have emerged in response, aiming at recycling and adding commercial value to the end products. The use of wastes can help diversify production and reduce final costs, in addition to providing alternative raw materials for a number of industrial sectors. The construction industry is one of the best targets of solid waste reconversion by virtue of the large amounts of raw materials it consumes and the large volume of final products in construction.

A variety of waste materials including construction rubble [1], tire rubber ash [2], blast furnace slag [3], silica fume [4], fly ash [5] and biological limestone [6] have been successfully tested in the preparation of dry mortars with proven advantages and beneficial effects over existing alternatives. Most of the new binder/aggregate admixtures improve the mechanical properties of mortar and allow the proportion of cement added to mortar to be reduced.

The granite cutting industry produces large amounts of wastes, solids (generated during extraction) and sludge (produced during transformation processes). Managing large amounts of sludge can be rather problematic for its producers, which must find appropriate places for storage and deposition. Dumping into rivers and lagoons is obviously not an environmentally safe solution and landfilling has serious drawbacks. Transporting and dumping of waste in landfills involves substantial costs; therefore, incorporating waste into other industrial processes could lead to a reduction of management costs and open up new business opportunities. Some previous studies have shown that granite sludge (GS) has a high potential as a raw material for the ceramic industry [7–14]. The morphological characteristics of this by-product [9–11,14] make it amenable to use as a filler in dry mortars. Moreover, its high content in iron oxides (coming from granite cutting with steel blades and abrasive metallic shot) can be used to prepare ceramic pigments, which constitutes one recent, attractive value added method for industrial wastes [15–18].

This work focused on the value of granite wastes (specifically, sludge residues derived from cutting of granite rocks) through their incorporation as alternative raw materials (fillers and/or red pigments) into cement-based mortar formulations. The chemical and mineralogical characteristics of GS, their transformation into ceramic pigment, and the physical and mechanical properties of the new formulated mortar were studied. These residues can replace ordinary limestone or act as pigments in mortar, the mechanical properties of which are retained or even improved.

2. Experimental

GS samples were supplied by *Granitos de los Pedroches S.A.* (Córdoba, Spain), a firm primarily engaged in ornamental rock cutting and polishing. This firm uses rocks of both national and foreign origin, the physico-chemical properties of which are somewhat differ-

* Corresponding author. Tel.: +34 957 218620; fax: +34 957 218621.
E-mail address: luis-sanchez@uco.es (L. Sánchez).

0958-9465/$ - see front matter © 2010 Elsevier Ltd. All rights reserved.
doi:10.1016/j.cemconcomp.2010.06.003

Table 1
Chemical composition (wt.%), density and specific surface area of the cements used in the masonry and plastering mortars studied.

Component	CEM II/A-V 42.5 R (masonry mortar)	BL I 52.5 N (plastering mortar)
SiO_2	26.96	21.50
Al_2O_3	9.65	4.00
Fe_2O_3	3.43	0.20
CaO	54.07	65.40
MgO	1.41	1.35
SO_3	3.22	3.60
K_2O	1.40	0.40
CaO free	1.03	1.50
Cl^-	0.01	0.006
Density (g/cm^3)	2.96	3.05
Specific surface area (Blaine) (m m/kg)	360	430

ent. This entailed studying a large number of GS samples (more than thirty, which was 1 month's worth of production). This ensured that the results would be representative of the average composition of the vast amount of rocks processed over such a long period.

The as-received GS samples, containing about 20–28% moisture, were dried at 110 °C to constant weight. In order to homogenize particle size, the samples were hand milled and passed through a 0.1 mm sieve before use as a mortar filler. The chemical composition of each GS sample was determined by X-ray fluorescence analysis (XRF) using a Philips PW2404 X-ray spectrometer.

Two different types of mortars were studied to evaluate the use of GS samples as pozzolan/filler admixtures in masonry mortar (UNE-EN-998-2) or pigment additives in plastering mortar (UNE-EN-998-1).

The components used to prepare standard mortars were Portland CEM II/A-V 42.5R type cement (the composition and fineness of which were those recommended by the mortar manufacturer CEMKOSA and shown in Table 1); natural silica and dolomite sands; and limestone (as filler). The SiO_2 used was of controlled grain size, with at least 90% of particles being less than 500 μm in size. Mineral limestone was a fine aggregate containing more than 98% $CaCO_3$. Two types of masonry mortar were prepared. The first series (samples A–D) was obtained simply by replacing some cement with GS; in the second (samples E–G), the limestone filler was increasingly replaced with GS. The composition of the seven samples is shown in Table 2.

Water/mortar ratios of 0.14 (samples A and B), 0.142 (samples C–E) and 0.15 (samples F and G), resulted in appropriate consistency (167 ± 2 mm; UNE-EN 1015-3) and acceptable workability. The air content of fresh mortars was 5 ± 1% [UNE-EN 1015-7]. All samples were cured at 25 °C and 50–90% relative humidity (RH). Compressive strength tests [UNE-EN 1015-11] were performed on prismatic specimens of size 40 × 40 × 160 mm that were examined after 28 days of curing.

The procedure specified in UNE EN 196-5 was used to determine pozzolanic activity. An amount of 20 g of test sample containing 80% of CEM-I and 20% of each pozzolan was mixed with 100 mL of distilled water. The samples thus obtained were allowed to stand in sealed plastic bottles that were placed in an oven at 40 °C for 8 days. Then, the samples were vacuum filtered and allowed to cool to ambient temperature in sealed Buchner funnels. The filtrates were analysed for [OH^-] by titration against dilute HCl with Methyl Orange as indicator, and for [Ca^{2+}] by adjusting the pH to 13 and titrating with EDTA in the presence of murexid as indicator. The results were plotted in a graph of [Ca^{2+}], in CaO equivalents (mmol L^{-1}) on the *y*-axis versus [OH^-], also in mmol L^{-1}, on the *x*-axis. The solubility curve for $Ca(OH)_2$ was then plotted and a control sample consisting of 100% CEM-I compared to ensure that the result lay on the same saturation curve. Any test results lying below such a line were assumed to indicate removal of Ca^{2+} from the solution and hence pozzolanic activity. On the other hand, any results lying on the line or above the line were taken to be indicative of no pozzolanic activity.

Table 2
Mortar formulations (wt.%).

Component	Samples								
	A	B	C	D	E	F	G	H	I
CEM II/A-V 42.5 R	10	9.5	9	8	10	10	10	–	–
BL I 52.5 N	–	–	–	–	–	–	–	13.5	13.5
SiO2	65	65	65	65	65	65	65	–	–
Dolomite	20	20	20	20	20	20	20	77	77
$CaCO_3$ filler[a]	5	5	5	5	4	3	–	9.5	–
GS [GS5[a]]	–	0.5	1	2	1	2	5	–	–
GS pigment	–	–	–	–	–	–	–	–	9.5

[a] Bulk density [UNE-EN 1097-3]: 0.88 and 0.56 g/cm^3 for $CaCO_3$ filler and *GS5*, respectively.

GS-pigment samples were obtained after heating GS samples at 700–900 °C for 4–24 h, using KNO_3 as a mineralizer in some cases. CIE $L^*a^*b^*$ colour parameters, obtained with a Perkin–Elmer colorimeter using a standard illuminant D, were used to differentiate samples in terms of colour. L^* was the lightness axis (black (0) → white (100)), a^* the green (−) → red (+) axis and b^* the blue (−) → yellow (+) axis. All measurements were made on powdered samples. A Lambda 2000 Perkin–Elmer spectrophotometer was used to obtain UV–Vis–NIR (ultraviolet–visible-near infrared) spectra over the 200–1400 nm range.

Coloured mortars were prepared by adding the GS pigment to white plastering mortar. The specific components used were Portland BLI 52.5 N cement, the composition and fineness of which are shown in Table 1; white dolomite sand; and limestone (filler). Coloured mortar was obtained simply by completely replacing the limestone filler with GS pigment (samples H and I). The composition of the two samples is shown in Table 2. Water/mortar ratios of 0.16 and 0.14 resulted in appropriate consistency and acceptable workability in the white and coloured mortars, respectively.

The mineralogical characterization and identification of crystalline phases was performed using X-ray diffraction (XRD) on a Siemens D5000 X-ray diffractometer using Cu Kα radiation. Particle size distribution was determined by laser diffraction, using a Mastersizer 2000LF from Malvern Instruments. Scanning electron microscopy (SEM) images were obtained with a Jeol JMS-6400 microscope.

3. Results and discussion

Table 3 shows the chemical composition of five GS samples which were representative of the set supplied by the manufacturer. As can be seen, the wastes had a high proportion of SiO_2 (52–62%) and Al_2O_3 (10.5–13.5%). Other significant components included Fe_2O_3 (6.8–27.9%) and CaO (3.4–5.9%). Iron in the waste came from the granite itself and was primarily the result of the common granite cutting practice, where an aqueous slurry consisting of $Ca(OH)_2$, stone powder and hard iron shot is continuously pumped and wets granite block slits. Even though the SiO_2/Al_2O_3/CaO proportion was similar for all samples, there were significant differences in iron content. This lack of uniformity can be ascribed to typology and composition differences between granite blocks. In any case, the amounts of Fe_2O_3 present were large enough to obtain an effective reddish pigment and greater than those previously reported for other granite wastes [8–13].

XRD patterns were similar for the thirty GS samples. Identical reflections were observed and differences in peak intensity were

Table 3
Chemical composition (wt.%) of selected GS samples as determined by XRF.

Sample	SiO_2	Al_2O_3	Fe_2O_3	MnO	MgO	CaO	Na_2O	K_2O	TiO_2	P_2O_5	L.O.I	Total
GS-1	61.76	13.38	6.85	0.08	1.87	5.90	2.35	3.45	0.50	0.16	2.89	99.19
GS-2	61.52	13.53	8.75	0.08	1.01	5.73	2.56	3.18	0.46	0.18	2.18	99.17
GS-3	61.93	12.80	12.41	0.11	0.73	4.59	2.54	3.59	0.31	0.18	0.02	99.22
GS-4	58.57	12.01	16.36	0.14	0.59	5.68	2.41	3.29	0.31	0.16	0.13	99.66
GS-5	51.98	10.50	27.89	0.22	0.58	3.44	2.02	2.99	0.27	0.15	0.01	100.06

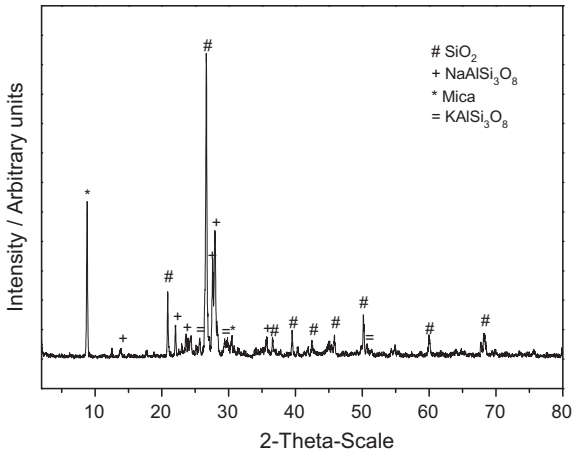

Fig. 1. XRD pattern for sample GS-3.

very subtle. By way of example, Fig. 1 shows the XRD pattern for sample GS-3. Quartz (SiO_2), sodium feldspar ($NaAlSi_3O_8$) and mica were present as main mineral phases, potassium feldspar ($KAlSi_3O_8$), biotite and calcite ($CaCO_3$) being the minor compounds. Despite the high iron content determined by XRF analysis (e.g. 12.4% for sample GS-3), no peaks for Fe, FeO(OH) or Fe_2O_3 phases were detected, probably because of their very poor crystallinity.

Fig. 2a shows the particle size distribution of selected samples as determined by laser diffraction. The wastes contained about 80% of particles with a diameter of 2–60 μm. The particles smaller than 2 μm (around 15%) were largely composed of clay minerals [14]. One specifically interesting result was the increase in the large particle size fraction with increasing iron content; this suggests that iron-based compounds are the main components of this fraction. As can be seen from Fig. 2b, the GS wastes exhibited a similar particle size distribution as the $CaCO_3$ mortar filler – which was supplied by CEMKOSA–; thus, the curves overlapped over ca. 80% of their areas. This supports the use of GS samples as a mortar filler. SEM images confirmed the particle size distribution results,

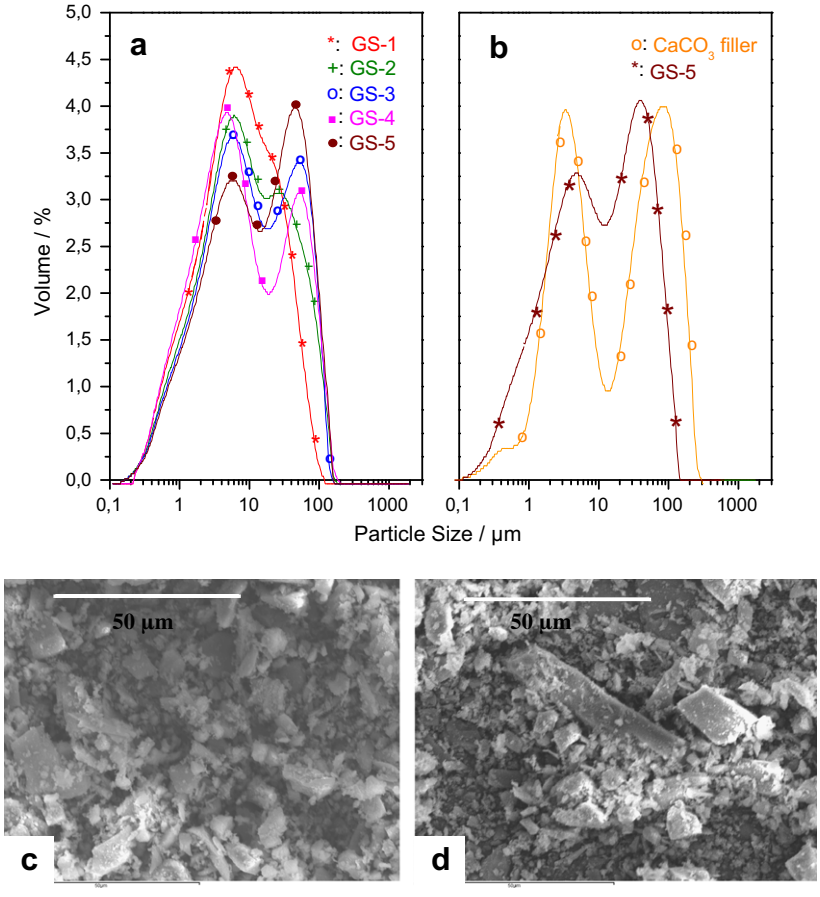

Fig. 2. Particle size distribution of: (a) GS samples and (b) $CaCO_3$ filler. SEM images of samples (c) GS-1 and (d) GS-5.

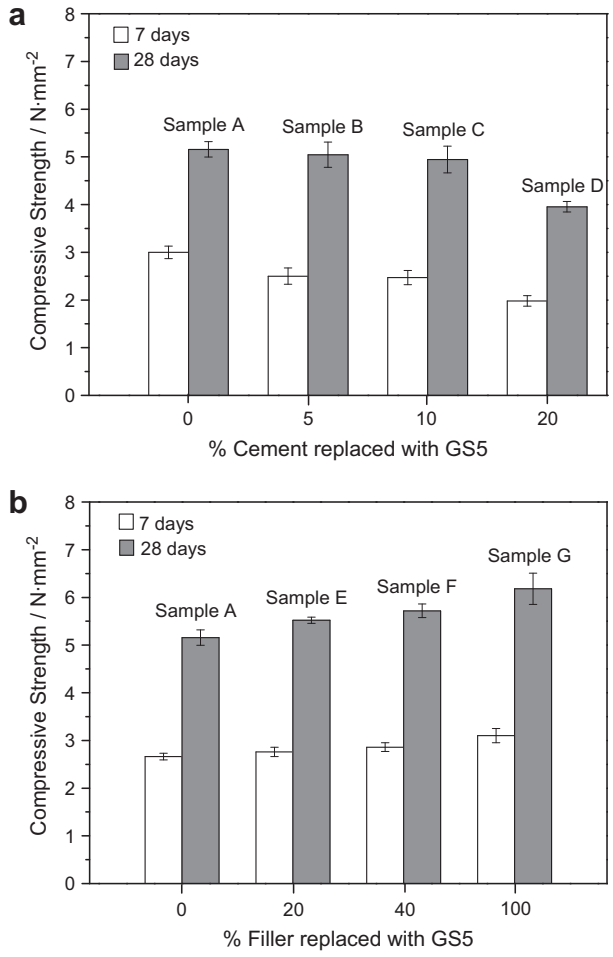

Fig. 3. Compressive strength after 7 and 28 days of curing in mortars where (a) cement or (b) filler were replaced with GS5.

the samples with the highest iron contents being those with coarser grains (see Fig. 2c and d).

On the other hand, based on the GS chemical analysis, these granite wastes can be expected to have pozzolanic activity on the basis of their contents in argillaceous minerals [19–20]. A simple test to assess their potential in this respect was performed by replacing small amounts of cement with GS5 (see Tables 2 and 3). The compressive strength of the resulting mansory mortars is shown in Fig. 3a. As can be seen, strength was retained even at high cement/GS ratios (samples B and C), but decreased significantly when more than 10% cement was replaced (sample D). Thus, this mechanical property of these short time cured mortars is not adversely affected by low GS to cement substitution ratios, which is suggestive of pozzolanic activity in these wastes. Even though the ultimate strength is developed over a long period in materials containing pozzolanic admixtures, at such an early age (28 days of curing) the beneficial effect in strength resulting from the pozzolanic reaction is substantial if a small amount of cement is replaced with pozzolanic material (as in samples B and C), consistent with previous findings [20–23]. The existence of pozzolanic activity was confirmed by measuring the Ca^{2+} and OH^- concentrations in a solution containing CEM-I and GS wastes, with values of 6.9

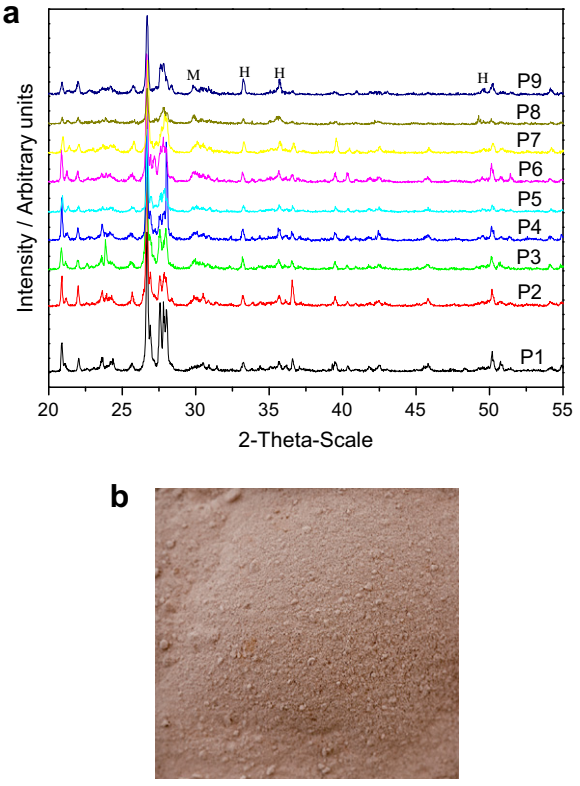

Fig. 4. (a) XRD patterns for GS pigments P1–P9 [M: magnetite, H: hematite]. (b) Photograph of P-9 powders.

Table 4
Heating conditions used in the preparation of GS-pigment samples and their colour coordinates.

GS pigment	GS precursor	Temperature (°C)	Time (h)	KNO_3[a] (%)	$L^*/a^*/b^*$
P1	GS-5	700	4	–	67.1/4.5/11.8
P2	GS-5	700	24	–	67.0/4.7/11.8
P3	GS-5	700	24	3	66.8/4.7/11.9
P4	GS-5	800	4	–	66.9/4.3/11.5
P5	GS-5	800	24	–	67.4/4.6/11.4
P6	GS-5	800	24	3	68.2/4.7/11.6
P7	GS-5	900	4	–	66.4/4.7/11.2
P8	GS-5	900	24	–	60.8/5.9/11.3
P9	GS-5	900	24	3	56.1/2.5/6.9
P10	GS-1	700	4	–	68.1/3.7/13.0
P11	GS-1	900	24	3	60.6/4.8/10.7

[a] Weight per cent in relation to Fe_2O_3 content of GS sample.

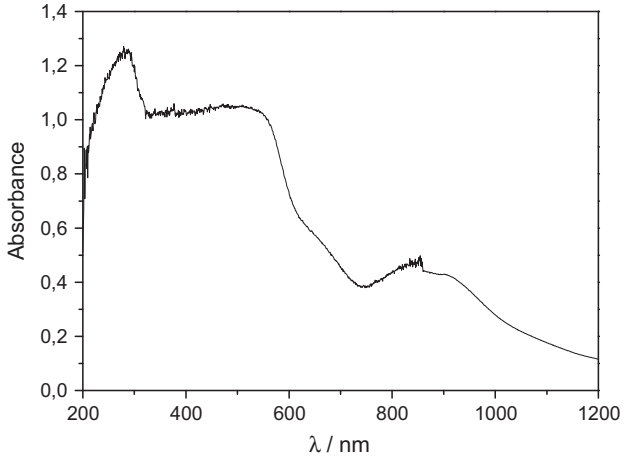

Fig. 5. UV–Vis–NIR spectra for standard hematite powder.

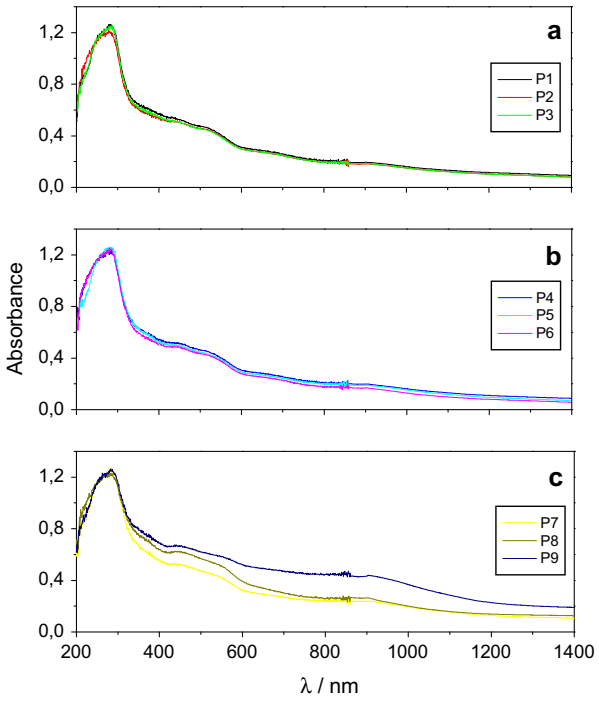

Fig. 6. UV–Vis–NIR spectra for GS pigments obtained at: (a) 700, (b) 800 and (c) 900 °C.

and 43.1 mmol L^{-1}, respectively. Even more interesting results were obtained by replacing the $CaCO_3$ filler with GS5 (samples E–G in Fig. 3b). Thus, a measurable improvement in compressive strength was observed with increasing replacement of the filler. The values measured at 28 days changed from 5.20 N mm^{-2} for sample A (with $CaCO_3$ filler) to 6.25 N mm^{-2} for sample G (with GS filler). The intrinsic rheological properties and pozzolanic activity of GS wastes may account for this beneficial effect.

An additional benefit of using these GS wastes results from their value as pigment additives, obtained by converting their iron content into coloured iron oxides. For this purpose, sample GS5, which was that with the highest iron content, was thermally treated at different temperatures for 4 or 24 h (see Table 4). This treatment produced iron oxides as revealed by XRD patterns (Fig. 4a). In addition to the diffraction lines assigned to quartz and feldspar as the main phases, the hematite peaks were clearly apparent, especially in the sample treated with the mineralizer at 900 °C; this phase was responsible for the reddish colour (Fig. 4b). One other iron oxide potentially formed under these conditions, magnetite (Fe_3O_4), was more difficult to detect with accuracy because some of its peaks overlapped with those of potassium feldspar ($KAlSi_3O_8$). The crystal phases obtained by heating at 700 or 800 °C are seemingly independent of the heating time and of whether a mineralizer is used.

Fig. 5 shows the UV–Vis–NIR spectra for standard hematite powder. As can be seen, they exhibit a strong band at 290 nm corresponding to the Fe-ligand charge exchange interaction. The other signals (viz. two shoulders at 580 and 662 nm and the broad band at 850 nm) can be assigned to the $^6A_{1g} \rightarrow {}^4A_{1g}$, $^6A_{1g} \rightarrow {}^4T_{2g}$ and $^6A_{1g} \rightarrow {}^4T_{1g}$ transitions typical of the octahedral Fe^{3+} ion in hematite [24]. The spectra for the pigments (Fig. 6) were similar except that the bands were weaker. The presence of KNO_3 increased band intensity throughout the absorption range and the bands were blurry. The colour coordinates for the pigments obtained from sample GS5 and GS1 (that with the lowest amount of Fe_2O_3), GS pigments P10 and P11, are shown in Table 4. The results correspond to a yellow–orange ($a^* = 4.5$, $b^* = 11$) middle intensity ($L^* = 67$) colour for pigments obtained at 700 and 800 °C. The samples became darker after prolonged calcination at a high temperature, and exhibited a brownish colour and decreased lightness ($L^* = 60.8$ for pigment P8). This effect was strengthened by the mineralizer ($L^* = 56.1$, $a^* = 2.5$, $b^* = 6.9$ for pigment P9). The darkening in sample colour was associated with the irreversible formation of magnetite at high temperature [25,26]: $3\ Fe_2O_3 \rightarrow 2\ Fe_3O_4 + ½\ O_2$. No significant differences in $L^*a^*b^*$ coordinates between the pigments obtained from low–iron GS wastes (P10 and P11) were observed, which suggests that any type of GS waste can be effectively converted into pigment.

Mortar colour could be strengthened by wholly replacing the filler with pigment. This would require the prior knowledge of the changes in the morphological characteristics of the wastes upon calcination. Fig. 7 shows the particle size distribution of pigments P1–P9; as can be seen, they were rather similar to those of

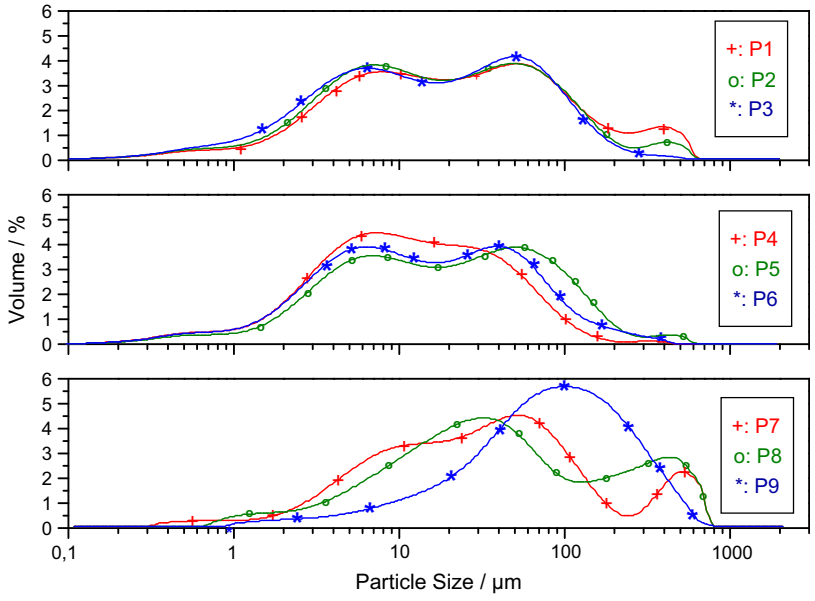

Fig. 7. Particle size distribution of GS pigments obtained at: (a) 700, (b) 800 and (c) 900 °C.

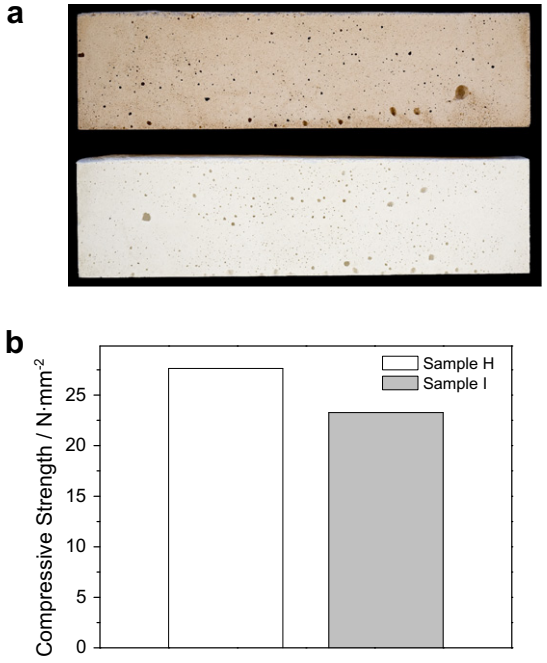

Fig. 8. (a) Photographs and (b) compressive strength after 28 days of curing in white (H) and coloured (I) mortars.

the high–iron GS samples. A small peak above 200 μm was observed due to the formation of large Fe_2O_3 particles, which was more marked in the pigments obtained at 900 °C. Pigment P9 exhibited a different particle size distribution curve with coarser grains resulting from the disappearance of feldspar particles and the crystallization of Fe_2O_3 and Fe_3O_4. Based on energy saving criteria, the best choice is clearly using pigment P1 as filler. The compressive strength values measured for the coloured plastering mortar thus formulated (Table 2, sample I; Fig. 8a) were close to those for the pristine mortar (sample H) and exceeded that recommended for this type of product in UNE-EN 998-1 (Fig. 8b).

4. Conclusions

The composition of granite sludge wastes, the main components of which are SiO_2, Al_2O_3, CaO and Fe_2O_3 based compounds, together with their small particle size warrant their use by the mortar industry. An interesting improvement in compressive strength was obtained by gradually replacing $CaCO_3$ filler with GS, increasing the compressive strength values from 5.2 to 6.25 N mm^{-2}. Conversely, 10% cement can be replaced with GS without loss of 28 d compressive strength. Both results support the use of GS wastes in mortar by virtue of their appropriate particle size distribution and potential pozzolanic activity. Moreover, GS can be readily converted into reddish pigments simply by calcination at 700–900 °C for a short time. The colour coordinates of the resulting products correspond to a middle–intensity yellow–orange colour due to Fe_2O_3 crystallizing during the after heating treatment. This is an additional benefit of these residues with a view to preparing coloured mortars with acceptable compressive strength.

Acknowledgements

This work was funded by Junta de Andalucía (Group FQM-175) and the firm CEMKOSA [Project: *"Estudio de viabilidad de la valorización de residuos procedentes del corte de piedras ornamentales (granito)"*].

References

[1] Álvarez Cabrera JL, Urrutia F, Lecusay D, Fernández A. Morteros de albañilería con escombros de demolición. Mater Constr 1997;47:43–8.
[2] Al-Akhras NM, Smadi MM. Properties of tire rubber ash mortar. Cem Concr Compos 2004;26:821–6.
[3] Cerulli T, Pistolesi C, Maltese C, Salvioni D. Durability of traditional plasters with respect to blast furnace slag-based plaster. Cem Concr Res 2003;33:1375–83.
[4] Rao GA. Investigations on the performance of silica fume-incorporated cement pastes and mortars. Cem Concr Res 2003;33:1765–70.
[5] Li G, Wu X. Influence of fly ash and its mean particle size on certain engineering properties of cement composite mortars. Cem Concr Res 2005;35:1128–34.
[6] Ballester P, Mármol I, Morales J, Sánchez L. Use of limestone obtained from waste of the mussel cannery industry for the production of mortars. Cem Concr Res 2007;37:559–64.
[7] Hernández-Crespo MS, Rincón JM. New porcelainized stoneware materials obtained by recycling of MSW incinerator fly ashes and granite sawing residues. Ceram Int 2001;27:713–20.
[8] Monteiro SN, Peçanha LA, Vieira CMF. Reformulation of roofing tiles body with addition of granite waste from sawing operations. J Eur Ceram Soc 2004;24:2349–56.
[9] Torres P, Fernandes HR, Agathopoulos S, Tulyaganov DU, Ferreira JMF. Incorporation of granite cutting sludge in industrial porcelain tile formulations. J Eur Ceram Soc 2004;24:3177–85.
[10] Vieira CMF, Soares TM, Sánchez R, Monteiro SN. Incorporation of granite waste in red ceramics. Mater Sci Eng A – Struct 2004;373:115–21.
[11] Menezes RR, Ferreira HS, Neves GA, Lira HL, Ferreira HC. Use of granite sawing wastes in the production of ceramic bricks and tiles. J Eur Ceram Soc 2005;25:1149–58.
[12] Acchar W, Vieira FA, Hotza D. Effect of marble and granite sludge in clay materials. Mater Sci Eng A – Struct 2006;419:306–9.
[13] Torres P, Manjate RS, Quaresma S, Fernandes HR, Ferreira JMF. Development of ceramic floor tile compositions based on quartzite and granite sludges. J Eur Ceram Soc 2007;27:4649–55.
[14] Torres P, Fernandes HR, Olhero S, Ferreira JMF. Incorporation of wastes from granite rock cutting and polishing industries to produce roof tiles. J Eur Ceram Soc 2009;29:23–30.
[15] Costa G, Della VP, Ribeiro MJ, Oliveira APN, Monrós G, Labrincha JA. Synthesis of black ceramic pigments from secondary raw materials. Dyes Pigments 2008;77:137–44.
[16] Legodi MA, de Waal D. The preparation of magnetite, goethite, hematite and maghemite of pigment quality from mill scale iron waste. Dyes Pigments 2007;74:161–8.
[17] Lazău RI, Păcurariu C, Becherescu D, Ianoş R. Ceramic pigments with chromium content from leather wastes. J Eur Ceram Soc 2007;27:1899–903.
[18] Berry FJ, Costantini N, Smart LE. Synthesis of chromium-containing pigments from chromium recovered from leather waste. Waste Manage 2002;22:761–72.
[19] Türkmenoglu AG, Tankut A. Use of tuffs from central Turkey as admixture in pozzolanic cements: assessment of their petrographical properties. Cem Concr Res 2002;32:629–37.
[20] Lavat AE, Trezza MA, Poggi M. Characterization of ceramic roof tile wastes as pozzolanic admixture. Waste Manage 2009;29:1666–74.
[21] Lee T-C, Rao M-K. Recycling municipal incinerator fly- and scrubber-ash into fused slag for the substantial replacement of cement in cement-mortars. Waste Manage 2009;29:1952–9.
[22] Rodríguez de Sensale G. Strength development of concrete with rice-husk ash. Cem Concr Comp 2006;28:158–60.
[23] Cyr M, Lawrence P, Ringot E. Efficiency of mineral admixtures in mortars: quantification of the physical and chemical effects of fine admixtures in relation with the compressive strength. Cem Concr Res 2006;36:264–77.
[24] Lever AB. Studies in physical and theoretical chemistry inorganic electronic spectroscopy. Amsterdam: Elsevier; 1986.
[25] García A, Llusar M, Badenes J, Tena MA, Monrós G. Encapsulation of hematite in zircon by microemulsion and sol–gel methods. J Sol–Gel Sci Technol 2003;27:267–75.
[26] García A, Sorlí S, Calbo J, Tena MA, Monrós G. Effect of the surfactant and precipitant on the synthesis of pink koral by microemulsion. J Eur Ceram Soc 2003;23:1829–38.